American Mineralogist, Volume 107, pages 377–384, 2022

Characterization of carbon phases in Yamato 74123 ureilite to constrain the meteorite shock history

Anna Barbaro[1,*], Fabrizio Nestola[2,3], Lidia Pittarello[4], Ludovic Ferrière[4], Mara Murri[5], Konstantin D. Litasov[6], Oliver Christ[2], Matteo Alvaro[1], and M. Chiara Domeneghetti[1]

[1]Department of Earth and Environmental Sciences, University of Pavia, Via A. Ferrata 1, I-27100 Pavia, Italy
[2]Department of Geosciences, University of Padova, Via Gradenigo 6, 35131 Padova, Italy
[3]Geoscience Institute, Goethe-University Frankfurt, Altenhöferallee 1, 60323 Frankfurt, Germany
[4]Department of Mineralogy and Petrography, Natural History Museum, Burgring 7, 1010 Vienna, Austria
[5]Department of Earth and Environmental Sciences, University of Milano-Bicocca, I-20126 Milano, Italy
[6]Vereshchagin Institute for High Pressure Physics RAS, Troitsk, Moscow, 108840 Russia

Abstract

The formation and shock history of ureilite meteorites, a relatively abundant type of primitive achondrites, has been debated for decades. For this purpose, the characterization of carbon phases can provide further information on diamond and graphite formation in ureilites, shedding light on the origin and history of this meteorite group. In this work, we present X-ray diffraction and micro-Raman spectroscopy analyses performed on diamond and graphite occurring in the ureilite Yamato 74123 (Y-74123). The results show that nano- and microdiamonds coexist with nanographite aggregates. This, together with the shock-deformation features observed in olivine, such as mosaicism and planar fractures, suggest that diamond grains formed by a shock event (≥15 GPa) on the ureilitic parent body (UPB). Our results on Y-74123 are consistent with those obtained on the NWA 7983 ureilite and further support the hypothesis that the simultaneous formation of nano- and microdiamonds with the assistance of a Fe-Ni melt catalysis may be related to the heterogeneous propagation and local scattering of the shock wave. Graphite geothermometry revealed an average recorded temperature (T_{max}) of 1314 °C (±120 °C) in agreement with previously estimated crystallization temperatures reported for graphite in Almahata Sitta ureilite.

Keywords: Carbon phases, diamond, graphite, ureilite meteorites, shock, impact event

Introduction

Ureilites represent the second largest group of achondrite meteorites (Goodrich 1992), with about 570 individuals with distinct names but only six observed falls (Meteoritical Bulletin Database 2020). Their formation, origin, and history are still under discussion among the scientific community. The debate about the formation of carbon phases contained in these meteorites has been going on for 80 years (see Nestola et al. 2020, and references therein).

As reported by Goodrich (1992), ureilites appear to be fractionated ultramafic igneous rocks, either magmatic cumulates (Berkley et al. 1980; Goodrich et al. 1987) or partial melt residues (Boynton et al. 1976; Scott et al. 1992) and, thus, the products of planetary differentiation processes. These conclusions were based on mineralogy, textures, fabrics, lithophile element chemistry, and on some aspects of Sm-Nd isotopic systematics (Berkley et al. 1976) observed in these meteorites (Goodrich 1992). Ureilites strongly differ from the other groups of stony meteorites (i.e., due to a high content of carbon phases and distinct oxygen isotopic composition) and, compared to chondrites, they are enriched in Mg but depleted in metal, troilite, and alkalis. Ureilites typically contain large olivine grains and a few smaller low-Ca-clinopyroxene (pigeonite) aggregates in a fine-grained, carbon-rich matrix. Minor phases are kamacite (1–3 vol% with the Ni content up to 7.3%), troilite (1–2%), chromite (1–2%), and carbon material (up to 8.5%) (Cloutis et al. 2010; Goodrich et al. 2015). Carbon is present as diamond, usually with stacking disorder and nanotwins (Németh et al. 2014, 2020a, 2020b; Salzmann et al. 2015; Murri et al. 2019), graphite, and organic material (e.g., Sabbah et al. 2010).

The different shock levels observed in ureilites are very important for constraining their history. Shock level determination in meteorites was first proposed by Stöffler et al. (1991, 2018) and is subdivided in six stages of shock for ordinary chondrites, from low (S1) to high (S6) level of shock, based on: (1) shock effects in olivine and plagioclase (e.g., extinction, fractures, planar elements), and (2) the presence of glass and/or of high-pressure silicate phases. Recently, Nakamuta et al. (2016) adapted the shock classification based on olivine in chondrites to the observations in ureilites. For this reason, we will apply this classification in this work.

The occurrence of diamonds in ureilites poses the question of how this high-pressure mineral formed and whether diamonds in ureilites are similar or not to those formed by shock in terrestrial impact structures (e.g., Masaitis 1998; Hough et al. 1995; Koeberl

* E-mail: anna.barbaro01@universitadipavia.it

0003-004X/22/0003–377$05.00/DOI: https://doi.org/10.2138/am-2021-7856

et al. 1997; Ohfuji et al. 2015; Murri et al. 2019). Three main hypotheses have been proposed for the formation of diamonds in ureilites: (1) static high-pressure conditions in the deep interior of large parent bodies (Urey 1956); (2) direct transformation from graphite due to shock (e.g., Lipschutz 1964; Bischoff et al. 1999; Grund and Bischoff 1999; Nakamuta and Aoki 2000, 2016; Hezel et al. 2008; Le Guillou et al. 2010; Ross et al. 2011; Lorenz 2019), also strongly supported by De Carli (1995) and De Carli et al. (2002); and (3) growth from a dilute gas phase, i.e., at low pressure in the solar nebula by a chemical vapor deposition (CVD) process (Fukunaga et al. 1987). The hypothesis of formation under static high-pressure conditions was recently supported by Miyahara et al. (2015) and Nabiei et al. (2018), who concluded that the size of a hypothetical ureilitic parent body (UPB) could be comparable to the size of Mars since static high-pressure conditions would be required for the formation of micrometer-scaled-diamond crystallites. The shock hypothesis was instead supported by the results obtained by Nakamuta et al. (2016). Indeed, these authors proposed that diamonds in ureilites could have formed at high-pressure (above 12 GPa) by spontaneous shock transformation from graphite and at low pressure (6–10 GPa) by a solid-state catalytic transformation from graphite in presence of a Fe-Ni melt. Additional support to the shock hypothesis is provided in a recent work by Nestola et al. (2020) on Almahata Sitta samples (AhS 72 and AhS 209 b), as well as on NWA 7983. In their study, graphite associated with nano- and (in NWA 7983) microdiamonds was reported, suggesting that the conversion from graphite to diamond was triggered by an impact event and was favored by the catalytic effect of Fe-Ni melts.

Yamato 74123 (Y-74123) ureilite is a meteorite that was found in Antarctic in 1974 by the Japanese expedition on the Yamato mountains. The first detailed study of Y-74123 dates back to 1978, when Hintenberger et al. (1978) measured its noble gas contents as well as several major and minor element bulk rock abundances. Takeda et al. (1980) have reported the petrological description and a chemical characterization of pyroxenes, which revealed Fe-bearing augite compositions ($En_{75}Fs_{18}Wo_7$). In addition, the magnetic properties of Y-74123 were studied by Nagata (1980). Moreover, Grady et al. (1985) carried out a C-isotopic study on Y-74123 reporting values of about $\delta^{13}C_{PDB} = -1.7$, well inside the range of ureilites. However, the carbon phases of Y-74123 have not been extensively studied yet.

In this work, we present the results of a multi-methodological study carried out on diamond and graphite aggregates observed in Yamato 74123 to understand the carbon phases formation in ureilites. In addition, a comparison with similar carbon phases in other meteorites, based on a literature survey and a discussion on their possible formation hypothesis, are also presented.

Methods

The fragment of Y-74123 (NHMV-#7636_A) and a corresponding polished thin section (NHMV-L9822) investigated in this study were kindly provided by the Natural History Museum Vienna (Austria). The thin section was investigated by optical and electron microscopy at the Department of Earth and Environmental Sciences, University of Pavia (Italy). Scanning electron microscopy (SEM) of the uncoated fragment of Y-74123 was performed using a FEI Quanta 200 SEM equipped with an energy-dispersive X-ray spectrometry (EDS) in low-vacuum mode at the Centro di Analisi e Servizi per la Certificazione (CEASC) of the University of Padova (Italy). Backscattered electron (BSE) images of Y-74123 were obtained in low-vacuum mode analytical conditions, at the working distance of 10.6 mm, with an emission current of 93 mA, and a voltage of 20 kV, with the aim to identify the graphite beds in which diamonds were probably located. The BSE images collected by SEM were merged and analyzed with ImageJ and MultiSpec software to estimate the relative percentages of each phase of interest observed on the surface of the investigated meteorite fragment.

Carbon phases were manually extracted from the fragment and mounted on the tip of a 100 µm diameter glass fiber (Fig. 1) and investigated using micro-Raman spectroscopy (MRS) followed by X-ray diffraction (XRD).

Micro-Raman spectroscopy analyses were performed on the graphite material occurring in the extracted carbon-bearing subsample of Figure 1 to estimate the recorded temperature using the geothermometer of Cody et al. (2008), modified by Ross et al. (2011). The analysis of Y-74123 graphite was performed by high-resolution MRS using a Horiba LabRam HR Evolution spectrometer equipped with an Olympus BX41 confocal microscope at the controlled temperature of 20 (±1) °C at the Department of Earth and Environmental Sciences of the University of Pavia. A 532 nm laser excitation with an operating power of 1–2 mW (to prevent damage to the graphite), a grating of 600 g/mm, and a magnification of 50× were used. The spectrometer was calibrated using the silicon Raman peak at 520.5 cm^{-1}. The spectral resolution was 2 cm^{-1} and the acquisition time for each spectrum was 30 s with four accumulations. Curve fitting of the spectra was carried out using the OMNIC software for dispersive Raman (Thermo-Fisher Scientific) adopting Gaussian + Lorentzian curves to obtain the best fit. XRD analyses were then performed on the same carbon-bearing subsample (Fig. 1) using a Rigaku-Oxford Diffraction Supernova κ-geometry goniometer with an X-ray Mo microsource equipped with a Pilatus 200 K Dectris detector in transmission mode, controlled by the CrysAlis-Pro software at the Department of Earth and Environmental Sciences in University of Pavia. Line profile analysis fitting of the obtained diffraction pattern was performed using the High Score Plus Software package (Panalytical) to estimate the crystallite size.

Results

Petrographic description and observation by scanning electron microscopy

The investigated polished thin section of Y-74123 consists of aggregates of subhedral to anhedral olivine mineral grains, with varying amounts of interstitial pyroxenes and Si-Al-rich glass. The sample contains coarse-grained olivine and minor pigeonite crystals, ranging from 0.1 to 1.5 mm in size, surrounded by a large amount of opaque material (Fig. 2), composed of carbon mixed with different sulfides and metal phases. Pores and small grains of metal and sulfide (≤100 µm in size) commonly occur in the interstitial space between pyroxene and olivine grains.

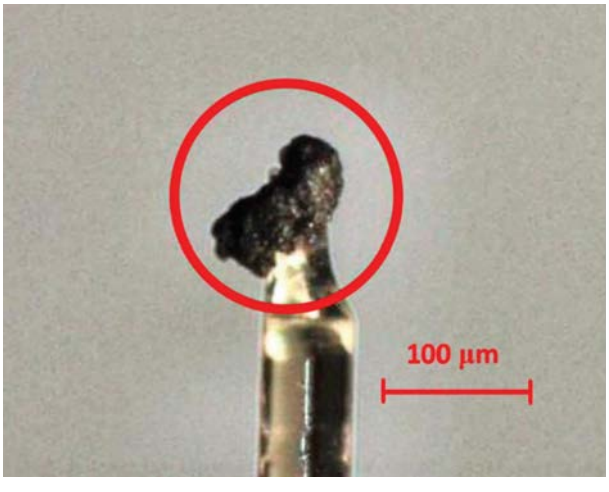

Figure 1. Carbon-bearing subsample of Y-74123 attached at the top of a glass fiber. Micro-Raman spectroscopy and XRD analyses were performed on this subsample. (Color online.)

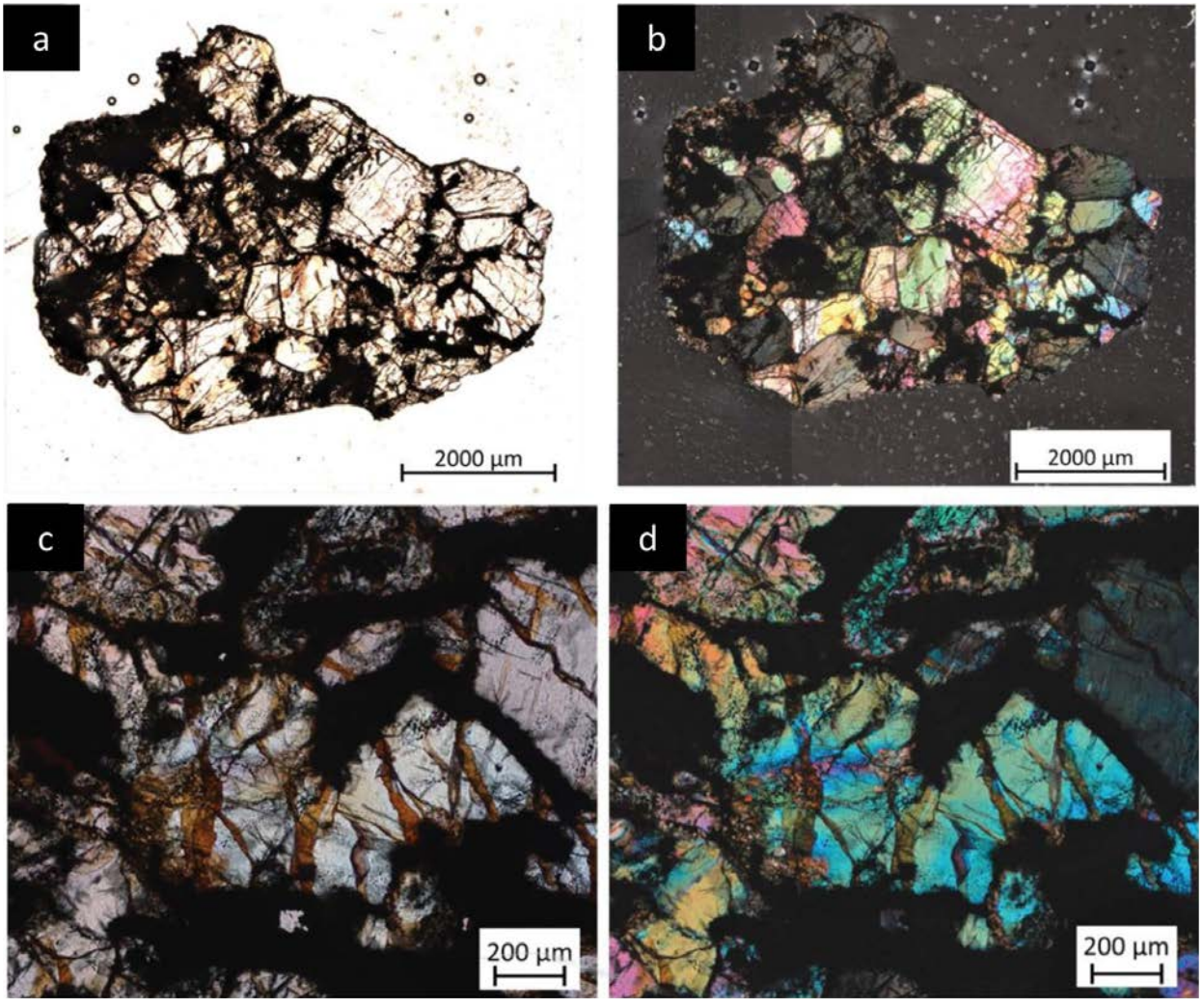

Figure 2. Yamato 74123 polished thin section (NHMV-L9822) overview in plane-polarized light (**a**) and between crossed polarizers (**b**); detailed structure of olivine grains in Y-74123 in plane-polarized light (**c**); and between crossed polarizers (**d**) are also presented. Note the presence of interstitial opaque material and the size of olivine grains, which dominate the thin section. (Color online.)

The shock level of Y-74123 was determined using optical microscope observations on shock microstructures in olivine crystals in transmitted light and following the criteria of Stöffler et al. (1991, 2018) and Nakamuta et al. (2016). Olivine crystals show undulate extinction, planar fractures, and, locally, mosaicism. The concurrent observation of undulate extinction and mosaicism in olivine indicates pressure in the range of 15–20 GPa, corresponding to shock level S4 (Stöffler et al. 2018). In addition, both silicates, i.e., olivine and clinopyroxene, show darkening caused by the dispersion of Fe-Ni metal and sulfides within the grains, which is commonly associated with shock metamorphism (e.g., Rubin 2006). In the investigated sample, even after a careful inspection by optical and electron microscopy, high-pressure polymorphs of olivine, such as wadsleyite or ringwoodite, were not found.

A fragment of Y-74123, about 8 × 5 × 5 mm in size, was analyzed by SEM. Figure 3a shows a BSE image of a typical carbon aggregate, which occurs as an interstitial phase in silicates. The size of the carbon phases in Y-74123 is evident in Figure 3b, where carbon phases are about 10 µm wide.

In Figure 3a, it is possible to see that locally, metal phases, indicated as "Fe-Ni metal," occur next to silicates. These metal phases are extremely fine-grained, partly mixed with the carbon phases.

The relative abundances, expressed in percentages, of the main mineralogical components present on the surface of the investigated sample of Y-74123 are 91% of silicate phases (olivine and pyroxene), 7% of carbon phases, and 2% of Fe-Ni metal and alloys, respectively (Fig. 4). The image analysis performed on the surface of the fragment of Y-74123 was important to find the best carbon aggregate zone from which to extract the carbon-bearing aggregate to be analyzed by MRS and XRD. The investigated fragment of Y-74123 turned out to be relatively easy to be cut and polished in comparison with many other studied ureilites, indicating a relatively low amount of diamonds.

X-ray diffraction

The reconstructed XRD image of the carbon-bearing aggregate of Yamato 74123 and its powder diffraction pattern are shown in Figures 5a and 5b. Instead, Figure 5c clearly shows the presence of spots referred to micrometer-sized diamond.

In particular, Figure 5a shows both rings and spots at *d*-spacing characteristic of cubic diamond (*d*-spacing at 2.06, 1.26, and 1.07 Å) and hexagonal graphite (highest peak at *d*-spacing at 3.34 Å, while the peaks at *d*-spacing 2.03 and 1.15 Å are overlapped by the diamond peaks). In Figure 5b, the highest peak of diamond (at *d*-spacing 2.06 Å) shows a slight asymmetry. This asymmetry could be ascribed, at higher *d*-spacing ($d \approx 2.18$ Å), to the presence of cubic and hexagonal sp^3 stacked layers or nanotwins (Murri et al. 2019) and, at lower *d*-spacing ($d \approx 2.02$ Å), to the main peak of Fe metal (which also shows peaks at *d*-spacing 1.42 and 1.17 Å). In addition to diamond, graphite, and Fe metal, a few other peaks can be assigned to troilite (*d*-spacing at 2.99, 2.66, 1.72, and 1.68 Å), and also to minor silicate matrix components. The presence of cubic Ni, common in ureilites, cannot be excluded, as its peaks overlap those of metallic Fe and troilite.

To estimate the crystallite size of the carbon phases, we applied line profile analysis fitting to the diffraction pattern reported in Figure 5b. The integral breadth values, which were obtained by this method, were then inserted into the Scherrer equation (Eqs. 1 and 2; Scherrer 1918) to estimate the crystallite size, as follows:

$$\beta(2\theta) = \frac{K_\beta \times \lambda}{\langle D \rangle_V \cos\theta_{hkl}} \quad (1)$$

$$\frac{D_V}{K_\beta} = \frac{\lambda}{\cos\theta_{hkl} \times \beta(2\theta)} \quad (2)$$

The Scherrer equation provides a correlation between peaks broadening β, the dimension of diffracted domain, and the crystallite size (D_V). K is a constant value ranging between 0.5 and 1, describing the contribution of crystallites shape and dependent upon the relative orientation of the scattering vector with respect to the external shape of the crystallite (Scherrer 1918).

For diamond, to obtain a reliable estimate of the crystallite size, we only used the two peaks at *d*-spacing 1.26 and 1.07 Å, as they do not exhibit any overlap with peaks of other phases within the analyzed carbon fragment. A similar approach was

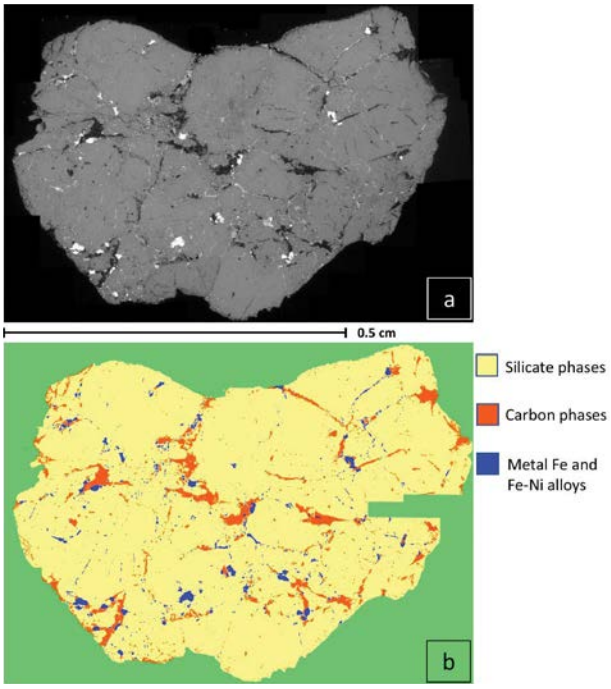

Figure 4. (**a**) BSE mosaic of the Yamato 74123 fragment (NHMV-7636_A) showing the typical texture of the meteorite. (**b**) Image analysis applied to **a** with the percentage referred to silicate phases, carbon phases, Fe-Ni metal, Fe-Ni alloys, and Fe-oxides. (Color online.)

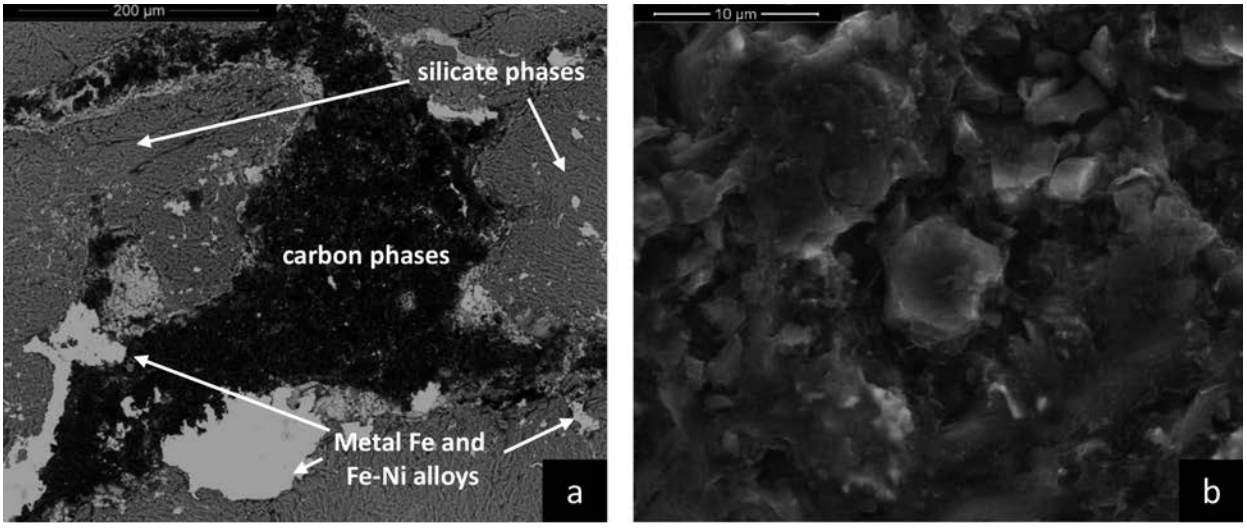

Figure 3. (**a**) BSE image of a carbon aggregate from which the investigated carbon-bearing subsample was extracted. Also note the presence of silicate phases and Fe-Ni metal and alloys (metal + troilite + oxide). (**b**) Detail of **a** in secondary electron (SE). As visible on this image, the aggregates in the carbon phases beds are not larger than 10 µm in size.

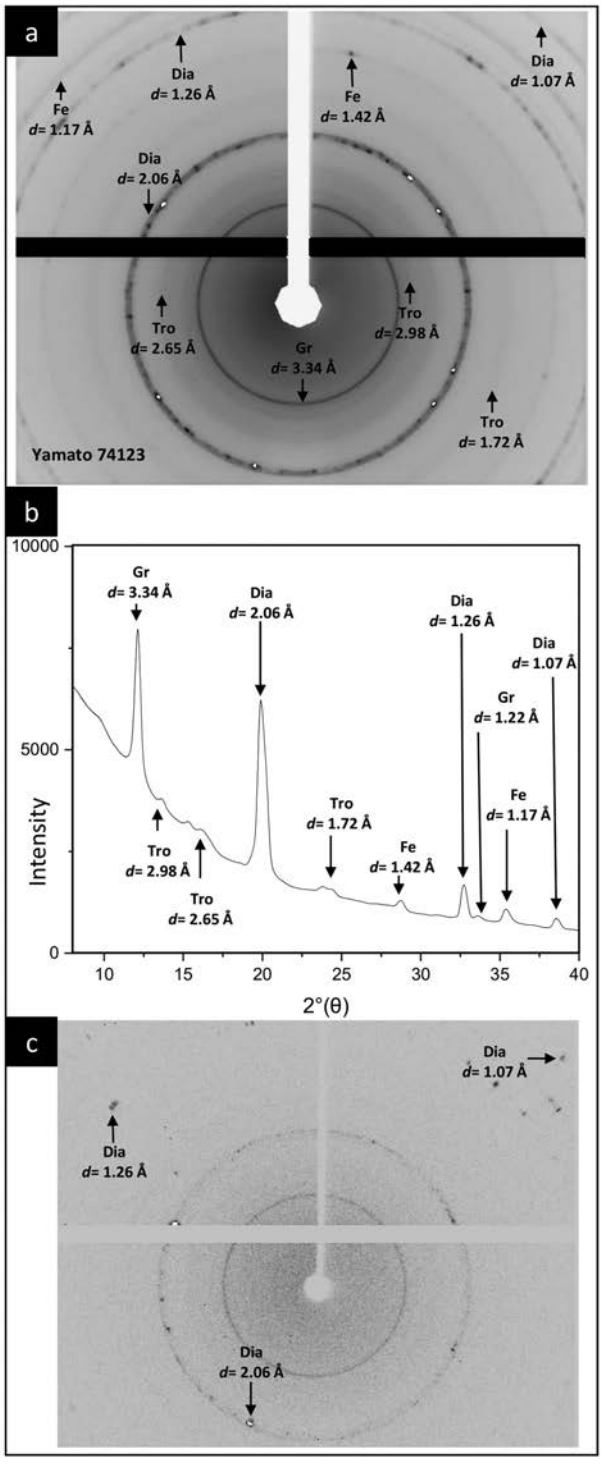

Figure 5. X-ray diffraction images of the carbon-bearing subsample from Y-74123. (**a**) Reconstructed powder diffraction image and (**b**) X-ray diffraction pattern of the investigated sample, analyzed by micro-X-ray powder diffraction are shown. The most abundant phases found in the carbon-bearing aggregate are diamond (Dia), graphite (Gr), Fe metal (Fe), and troilite (Tro). (**c**) A diffraction image shows the spots corresponding to micrometer-sized diamonds.

Table 1. The unit-cell parameters for the micrometer-sized cubic diamond single crystal found in Y-74123

Single-crystal micrometer-sized cubic diamond (space group *Fd$\bar{3}$m*)		
	a = 3.569(1) Å	
	V = 45.46(2) Å^3	
	Polycrystalline diamond	
Pos. (2θ°)	*d*-spacing (Å)	D_V (nm)
32.65	1.26	15
38.50	1.07	11
	Polycrystalline graphite	
Pos. (2θ°)	*d*-spacing (Å)	D_V (nm)
12.10	3.34	8

Notes: Mo λ ≈ 0.71. 2θ° positions of the graphite and diamond diffraction peaks, *d*-spacings, and the crystallite size (D_v) are reported. The crystallite size was calculated using the most intense peak of graphite at 3.34 Å, and the two peaks of diamond at 1.26 and 1.07 Å.

Table 2. Center positions for G, D, and D′ bands and FWHM (both in cm^{-1}) of Y-74123

G-band center	G-band FWHM	G-band FWHM corrected	D-band center	D-band FWHM	D′-band center	D′-band FWHM	T_{max} (°C)
			Y-74123				
1582	24	15	1356	49	1618	21	1286
1580	22	13	1354	46	1618	19	1310
1579	21	13	1349	37	1611	22	1329
1579	18	11	1356	22	1618	17	1365
1579	20	12	1351	40	1616	23	1334
1581	25	16	1350	50	1617	22	1265

Notes: Calculated crystallization temperature, T_{max}, is reported in the last column and was obtained using the Equation 3. The uncertainty on T_{max} is (2σ) ±120 °C.

used to estimate the crystallite size of graphite, using the peak at *d*-spacing 3.34 Å (see Table 1). The results are reported in Table 1, along with the unit-cell parameters and the space group for the diamond single crystal found in Y-74123. The possibility to estimate the unit-cell parameters for the investigated diamond in Y-74123 implies that micrometer-sized diamonds (i.e., spots in the diffraction image) are present. As it appears from the XRD images (Figs. 5a and 5c), i.e., on the basis of the presence of spots and rings, we can state that nanographite coexists with micro- and nanodiamonds in Y-74123, as also observed by Goodrich et al. (2020) and Nestola et al. (2020) in the NWA 7983 ureilite.

Micro-Raman spectroscopy

We applied the geothermometric approach by Cody et al. (2008) and Ross et al. (2011), following the same procedure as reported in Barbaro et al. (2020a, 2020b) for Almahata Sitta samples (AhS 209 b, AhS 72, and AhS A135A), to determine the T_{max} recorded by graphite. The temperature was estimated using Equation 3, expressed in terms of Raman G-band full-width at half maximum (FWHM) (Γ_G):

$$T_{max}(°C) = 1594.4 - 20.4\Gamma_G - 5.8 \times 10^{-2}\Gamma_G^2 \quad (3)$$

In Table 2, we list the graphite peaks positions (G, D, and D′ band), the relevant Γ_G values (G, D, and D′ bands FWHM) for Y-74123, as well as the T_{max} estimated using Equation 3.

To compare our Γ_G data with those published by Ross et al. (2011) and Barbaro et al. (2020b), we corrected our data for the instrumental peak broadening using a high-quality gem-quality lithospheric diamond (with Γ_G = 5 cm^{-1}), following the same procedure as in Ross et al. (2011) (see Table 2). In Table 2, for each set of acquisitions, the values of Γ_G used in Equation 3 to obtain the T_{max}, are reported. T_{max} values range between 1265 and

Table 3. Comparison among the T_{max} recorded by graphite in different ureilites using the geothermometer by Cody et al. (2008)[a]

	AhS 7 (Ross et al. 2011)	AhS 209 (Barbaro et al. 2020b)	AhS 72 (Barbaro et al. 2020b)	AhS (Barbaro et al. 2020b)	A135AY-74123 (This work)
Average T_{max} (°C)	990 ± 120	1266 ± 120	1242 ± 120	1332 ± 120	1314 ± 120

[a] See Cody et al. (2008) and Ross et al. (2011) for a detailed description of the applied geothermometry. The temperature values recorded by graphite in AhS 7 sample are after Ross et al. (2011) and those recorded for AhS 209, AhS 72, and AhS A135A are from Barbaro et al. (2020b).

1334 (±120) °C. These temperatures are slightly higher than those obtained by Ross et al. (2011) on graphite in AhS #7 ureilitic fragment (T_{max} of 990 ± 120 °C), whereas they are very similar to those obtained by Barbaro et al. (2020b) on other Almahata Sitta samples (average T_{max} of 1266 °C for graphite in AhS 209 b, 1242 °C in AhS 72, and 1332 °C in AhS A135A). A comparison between the average temperatures recorded by graphite on the above-quoted ureilitic samples is presented in Table 3.

Discussion

Micro-Raman spectroscopy and XRD analyses in Y-74123 revealed the presence of diamond and graphite aggregates in the interstitial space between silicate grains, as commonly observed in other ureilites (e.g., Hanneman et al. 1967; Vdovykin 1970). Our results from the XRD analysis on Y-74123 confirm the coexistence of nano- and microdiamonds associated with nanographite. In the carbon-bearing aggregates, we also detected Fe metal and troilite, which fill the interstitial space between graphite-diamond crystals or occur at the border of the carbon aggregates (Fig. 4).

The observed local differences in the size of the newly formed diamonds, i.e., nano- to micrometric, may result from heterogeneous shock distribution within a heterogeneous sample. The heterogeneous distribution of shock effects is mainly ascribed to shock impedance contrast between contiguous phases. For greater contrast, the shock impedance is amplified (Ogilvie et al. 2011), as in the case of large, "rigid," olivine crystals, separated by interstitial, relatively "soft," carbon-bearing matrix. This implies that the shock pressure locally experienced by the carbon phases might have been higher than that recorded by the adjacent olivine crystal, thus, explaining the local occurrence of relatively coarse-grained diamonds. Conversely, for cases of low contrast between phases, the shock impedance would have been suppressed. Furthermore, we cannot exclude that Y-74123 suffered multiple impact events with different *P-T* conditions.

Our study provides further evidence in support of the diamond formation mechanism in ureilites proposed for NWA 7983 ureilite by Nestola et al. (2020). According to this mechanism, the formation of micrometer-sized diamond crystals from graphite observed in Y-74123 is likely due to the combined effect of highly heterogeneous *P-T*-conditions due to shock wave propagation and immediate penetration of Fe-Ni melt into carbon aggregates, whereas the formation of nanodiamonds resulted from direct transformation from graphite (i.e., even without the catalytic Fe-Ni melt). The occurrence of Fe compounds, as observed in Y-74123, could explain the formation of diamonds at pressures ≥15–20 GPa (Nestola et al. 2020), which is lower than the pressure of 30–60 GPa estimated for diamonds formed in impact cratering processes on Earth (see, e.g., Koeberl et al. 1997 and references therein). In Nestola et al. (2020) it is clearly reported how the catalyzed formation of diamonds by metallic melts during a shock event can also account for the simultaneous formation of micro- and nanodiamonds in ureilites. These authors, with the aim to explain this process, reported an example of a pulsed heating experiment performed on a graphite-metal charge in a static high-pressure apparatus (Varfolomeeva 1971). This apparatus simulates natural impact processes (De Carli et al. 2002; Bundy and Kasper 1967), which produced diamonds up to 10 μm in size, found near to the catalyst, and nanodiamonds occurring in other parts of the experimental charge (Nestola et al. 2020 and references therein).

The proposed scenario is further supported by the average value of the temperatures determined for Y-74123 graphite [T_{max} = 1314 °C (±120 °C)], which is similar to the values reported by Barbaro et al. (2020a, 2020b) for Almahata Sitta samples (e.g., AhS 209 b, AhS 72, and AhS A135A), even though slightly higher than the values reported by Ross et al. (2011) for the AhS #7 sample. As reported by Gillet and El Goresy (2013), the shock peak temperature determination for a sample with a different mineral composition should also account for the effect of the porosity, grain boundaries, and heterogeneous composition of the rock. In addition, it is important to consider that the shock waves do not propagate at the same speed in all different minerals of a polymineralic rock, as explained above. However, even if it is difficult to estimate the exact peak shock pressure values of the impact event(s), we can argue that the temperature recorded by graphite may correspond to the shock-induced temperature or to a subsequent post-shock thermal event, as hypothesized by Gillet and El Goresy (2013). We exclude the possibility that our estimated temperature values could be a pre-shock temperature because our estimation is determined on newly crystallized nanographite. Such nanographite cannot be the pristine graphite of the UPB, which should have been micrometer-sized, due to the long residence time spent in the UPB deep interior. Therefore, as reported by Barbaro et al. (2020b) for three AhS ureilitic fragments, the nanographite formed by shock.

Implications

Our study on carbon phases in Yamato 74123 provides hints on the shock history of this specific meteorite, and generally, of the UPB. The XRD analysis carried out on Y-74123 showed that nanodiamonds coexist together with microdiamonds and nanographite, in agreement with observations by Nestola et al. (2020) on the NWA 7983 ureilite meteorite. In addition, by means of MRS analyses of graphite, we were able to show that: (1) the investigated sample exhibits homogeneous values of G-band centers (between 1579 and 1582 cm^{-1}) and D-band centers (between 1349 and 1356 cm^{-1}), and that (2) the Γ_G of graphite for the G-band range between 11 and 16 cm^{-1}. These values were used to estimate an average T_{max} of 1314 °C (±120 °C).

Our results support that micrometer-sized diamonds in Y-74123, as also suggested by Nestola et al. (2020) for

NWA 7983, formed with the assistance of the catalytic effect of metallic melts without requiring static high-pressures conditions within a large Mars-sized parent body. The formation of micro- and nanodiamonds and nanographite is likely to be the result of an impact event or multiple impact events. We assume that the temperature recorded by graphite, close to 1200–1300 °C, likely represents the shock-induced temperature excursion or corresponds to a subsequent post-shock temperature. The temperature values obtained in our sample Y-74123, together with further studies on ureilites, using the same approach as presented here, will contribute to widening our knowledge of the graphite resetting temperatures by shock.

In conclusion, the results from our combined SEM, XRD, and MRS study in Y-74123 suggest that one or multiple shock event(s), with the contribution of metallic melts catalysis, is likely responsible for the formation of diamond, both nano- and microdiamonds. Moreover, heterogeneity in the peak shock pressure that affected the UPB during the impact event(s) may also explain the coexistence of diamonds with notable different sizes.

Acknowledgments

This paper is dedicated to the memory of Heinrich Hintenberger (1910–1990), who donated to the NHM Vienna collection the Yamato 74123 sample used for this study. C.A. Goodrich is acknowledged for interesting discussions. S. Jaret and an anonymous reviewer are thanked for their comments, which greatly contributed to improving this manuscript. S. Redfern is thanked for editorial handling.

Funding

This work was supported by PNRA 2018 Grant number PNRA18 00247; A to F.N.; A.B., M.C.D., M.M., and M.A. were funded by the IMPACt project (R164WEJAHH) to M. Alvaro.

References cited

Barbaro, A., Domeneghetti, M.C., Goodrich, C.A., Meneghetti, M., Litti, L., Fioretti, A.M., Shaddad, M.H., Alvaro, M., and Nestola, F. (2020a) Shock temperature recorded by graphite in ureilites from Almahata Sitta. 51st Lunar and Planetary Science Conference, abstract 1480.

Barbaro, A., Domeneghetti, M., Goodrich, C., Meneghetti, M., Litti, L., Fioretti, A., Jenniskens, P., Shaddad, M., and Nestola, F. (2020b) Graphite based geothermometry on Almahata Sitta ureilites meteorites. Minerals, 10, 1005.

Berkley, J.L., Taylor, G.J., Keil, K., Harlow, G.E., and Prinz, M. (1980) The nature and origin of ureilites. Geochimica et Cosmochimica Acta, 44, 1579–1597.

Berkley, J.L., Brown, I.V., H.G., Keil, K., Carter, N.L., Mercier, J.-C.C., and Huss, G. (1976) The Kenna ureilite: an ultramafic rock with evidence for igneous, metamorphic, and shock origin. Geochimica et Cosmochimica Acta, 40, 1429–1437.

Bischoff, A., Goodrich, C.A., and Grund, T. (1999) Shock-induced origin of diamond in ureilites. 30th Annual Lunar and Planetary Science Conference, March 15–29, 1999, Houston, Texas, abstract 1100.

Boynton, W.V., Starzyk, P.M., and Schmitt, R.A. (1976) Chemical evidence for the genesis of the ureilites, the achondrite Chassigny and the nakhlites. Geochimica et Cosmochimica Acta, 40, 1439–1447.

Bundy, F.P., and Kasper, J.S. (1967) Hexagonal diamond—A new form of carbon. The Journal of Chemical Physics, 46, 3437–3446.

Cloutis, E.A., Hudon, P., Romanek, C.S., Bishop, J.L., Reddy, V., Gaffey, M.J., and Hardersen, P.S. (2010) Spectral reflectance properties of ureilites. Meteoritics & Planetary Science, 45, 1668–1611.

Cody, G.D., Alexander, C.M.O., Yabuta, H., Kilcoyne, A.L.D., Araki, T., Ade, H., Dera, P., Fogel, M., Militzer, B., and Mysen, B.O. (2008) Organic thermometry for chondritic parent bodies. Earth and Planetary Science Letters, 272, 446–455.

De Carli, P.S. (1995) Shock wave synthesis of diamond and other phases. Materials Research and Society Symposium Proceedings, 383, 21–31.

De Carli, P.S., Bowden, E., Jones, A.P., and Price, G.D. (2002) Laboratory impact experiments versus natural impact events. In Ch. Koeberl and K.G. MacLeod, Eds., Catastrophic Events and Mass Extinctions: Impacts and Beyond, Geological Society of America Special Paper 356, 595–605. Lunar and Planetary Institute.

Fukunaga, K., Matsuda, J., Nagao, K., Miyamoto, M., and Ito, K. (1987) Noble-gas enrichment in vapour-growth diamonds and the origin of diamond in ureilites. Nature, 328, 141–143.

Gillet, P., and El Goresy, A. (2013) Shock events in the Solar System: The message from minerals in terrestrial planets and asteroids. Annual Review of Earth and Planetary Sciences, 41, 257–285.

Goodrich, C.A. (1992) Ureilites: A critical review. Meteoritics, 27, 327–352.

Goodrich, C.A., Jones, J.H., and Berkley, J.L. (1987) Origin and evolution of the ureilite parent magmas: Multi-stage igneous activity on a large parent body. Geochimica et Cosmochimica Acta, 51, 2255–2273.

Goodrich, C.A., Hartmann, W.K., O'Brien, D.P., Weidenschilling, S.J., Wilson, L., Michel, P., and Jutzi, M. (2015) Origin and history of ureilitic material in the solar system: The view from asteroid 2008 TC_3 and the Almahata Sitta meteorite. Meteoritics & Planetary Science, 50, 782–809.

Goodrich, C.A., Nestola, F., Jakubek, R., Erickson, T., Fries, M., Fioretti, A.M., Ross, D.K., and Brenker, F.E. (2020) The origin of diamond in ureilites. 51st Lunar and Planetary Science Conference, abstract 1411.

Grady, M.M., Wright, I.P., Swart, P.K., and Pillinger, C.T. (1985) The carbon and nitrogen isotopic composition of ureilites: Implications for their genesis. Geochimica et Cosmochimica Acta, 49, 903–915.

Grund, T., and Bischoff, A. (1999) Cathodoluminescence properties of diamonds in ureilites: further evidences for a shock-induced origin. 62nd Annual Meteoritical Society Meeting, abstract 5074.

Hanneman, R.E., Strong, H.M., and Bundy, F.P. (1967) Hexagonal diamonds in meteorites: Implications. Science, 155, 995–997.

Hezel, D.C., Dubrovinsky, L., Nasdala, L., Cauzid, J., Simionovici, A., Gellissen, M., and Schonbeck, T. (2008) In situ micro-Raman and X-ray diffraction study of diamonds and petrology of the new ureilite UAE 001 from the United Arab Emirates. Meteoritics & Planetary Science, 43, 1127–1136.

Hintenberger, H., Jochum, K.P., Braun, O., Christ, P., and Martin, W. (1978) The Antarctic meteorite Yamato 74123—A new ureilite. Earth and Planetary Science Letters, 40, 187–193.

Hough, R.M., Gilmour, I., Pillinger, C.T., Arden, J.W., Gilkess, K.W.R., Yuan, J., and Milledge, H.J. (1995) Diamond and silicon carbide in impact melt rock from the Ries impact crater. Nature, 378, 41–44.

Koeberl, C., Masaitis, V.L., Shafranovsky, G.I., Gilmour, I., Langenhorst, F., and Schrauder, M. (1997) Diamonds from the Popigai impact structure, Russia. Geology, 25, 967–970.

Le Guillou, C., Rouzaud, J.N., Remusat, L., Jambon, A., and Bourot-Denise, M. (2010) Structures, origin and evolution of various carbon phases in the ureilite Northwest Africa 4742 compared with laboratory-shocked graphite. Geochimica et Cosmochimica Acta, 74, 4167–4185.

Lipschutz, M.E. (1964) Origin of Diamonds in the Ureilites. Science, 143, 1431–1434.

Lorenz, C.A., Shiryaev, A.A., Vlasov, I.I., and Borisovsky, S.E. (2019) Metamorphism of four desert ureilites and luminescence spectroscopy of defects in ureilitic diamonds. Meteoritics & Planetary Science, 54, 1197–1214.

Masaitis, V.L. (1998) Popigai crater: Origin and distribution of diamond-bearing impactites. Meteoritics & Planetary Science, 33, 349–359.

Meteoritical Bulletin Database (2020) Available: https://www.lpi.usra.edu/meteor/.

Miyahara, M., Ohtani, E., El Goresy, A., Lin, Y., Feng, L., Zhang, J.-C., Gillet, P., Nagase, T., Muto, J., and Nishijima, M. (2015) Unique large diamonds in a ureilite from Almahata Sitta 2008 TC 3 asteroid. Geochimica et Cosmochimica Acta, 163, 14–26.

Murri, M., Smith, R.L., McColl, K., Hart, M., Alvaro, M., Jones, A.P., Németh, P., Salzmann, C.G., Corà, F., Domeneghetti, M.C., and others (2019) Quantifying hexagonal stacking in diamond. Scientific Reports, 9, 10334.

Nabiei, F., Badro, J., Dennenwaldt, T., Oveisi, E., Cantoni, M., Hébert, C., Goresy, A., El, Barrat, J., and Gillet, P. (2018) A large planetary body inferred from diamond inclusions in a ureilite meteorite. Nature Communications, 9, 1327.

Nagata, T. (1980) Magnetic classification of Antarctic meteorites. Proceedings of the 21st Lunar and Planetary Science Conference, p. 1789–1799. Lunar and Planetary Science Institute, Houston, Texas.

Nakamuta, Y., and Aoki, Y. (2000) Mineralogical evidence for the origin of diamond in ureilites. Meteoritics & Planetary Science, 35, 487–493.

Nakamuta, Y., Kitajima, F., and Shimada, K. (2016) In situ observation, X-ray diffraction and Raman analyses of carbon minerals in ureilites: Origin and formation mechanisms of diamond in ureilites. Journal of Mineralogical and Petrological Sciences, 111, 252–269.

Németh, P., Garvie, L.A.J., Aoki, T., Dubrovinskaia, N., Dubrovinsky, L., and Buseck, P.R. (2014) Lonsdaleite is faulted and twinned cubic diamond and does not exist as a discrete material. Nature Communications, 5, 5447.

Németh, P., McColl, K., Smith, R.L., Murri, M., Garvie, L.A.J., Alvaro, M., Pécz, B., Jones, A.P., Corà, F., Salzmann, C.G., and McMillan, P.F. (2020a) Diamond-graphene composite nanostructures. Nano Letters, 20, 3611–3619.

Németh, P., McColl, K., Garvie, L.A.J., Salzmann, C.G., Murri, M., and McMillan, P.F. (2020b) Complex nanostructures in diamond. Nature Materials, 19, 1126 –1131.

Nestola, F., Goodrich, C.A., Morana, M., Barbaro, A., Jakubek, R.S., Chris, O., Brenker, F.E., Domeneghetti, M.C., Dalconi, M.C., Alvaro, M., and others (2020) Impact shock origin of diamond in ureilite meteorites. Proceedings of the National Academy of Sciences, 117, 25310–25318. https://doi.org/10.1073/

pnas.1919067117.
Ogilvie, P., Gibson, R.L., Reimold, W.U., Deutsch, A., and Hornemann, U. (2011) Experimental investigation of shock metamorphic effects in a metapelitic granulite: The importance of shock impedance contrast between components. Meteoritics & Planetary Science, 46, 1565–1586.
Ohfuji, H., Irifune, T., Litasov, K.D., Yamashita, T., Isobe, F., Afanasiev, V.P., and Pokhilenko, N.P. (2015) Natural occurrence of pure nano-polycrystalline diamond from impact crater. Scientific Reports, 5, 14702.
Ross, A.J., Steele, A., Fries, M.D., Kater, L., Downes, H., Jones, A.P., Smith, C.L., Jenniskens, P.M., Zolensky, M.E., and Shaddad, M.H. (2011) MicroRaman spectroscopy of diamond and graphite in Almahata Sitta and comparison with other ureilites. Meteoritics & Planetary Science, 46, 364–378.
Rubin, A. (2006) Shock, post-shock annealing, and post-annealing shock in ureilites. Meteoritics & Planetary Science, 41, 125–133.
Sabbah, H., Morrow, A.L., Jenniskens, P., Shaddad, M.H., and Zare, R.N. (2010) Polycyclic aromatic hydrocarbons in asteroid 2008 TC_3: Dispersion of organic compounds inside asteroids. Meteoritics & Planetary Science, 45, 1710–1717.
Salzmann, C.G., Murray, B.J., and Shephard, J.J. (2015) Extent of stacking disorder in diamond. Diamond and Related Materials, 59, 69–72.
Scherrer, P. (1918) Estimation of the size and internal structure of colloidal particles by means of röntgen. Journal of Mathematical Physics, 2, 98–100.
Scott, E.R.D., Keil, K., and Taylor, G.J. (1992) Origin of ureilites by partial melting and explosive volcanism on carbon-rich asteroids. Proceedings of the 23rd Lunar and Planetary Science Conference, pp. 1253–1254.
Stöffler, D., Keil, K., and Edward, R.D.S. (1991) Shock metamorphism of ordinary chondrites. Geochimica et Cosmochimica Acta, 55, 3845–3867.
Stöffler, D., Hamann, C., and Metzler, K. (2018) Invited Review Shock metamorphism of planetary silicate rocks and sediments: Proposal for an updated classification system. Meteoritics & Planetary Science, 49, 5–49.
Takeda, H., Mori, H., Keizo, Y., and Shiraishi, K. (1980) Mineralogical examination of the Allan Hills achondrites and their bearing on the parent bodies. Memoirs of National Institute of Polar Research. Special Issue, 17, 119–144.
Urey, H.C. (1956) Diamond, meteorites, and the origin of the solar system. The Astrophysical Journal, 124, 623–637.
Varfolomeeva, T.D. (1971) Synthesis and investigation of polycrystalline diamond. Ph.D. thesis, Institute for High Pressure Physics, USSR Academy of Sciences, 154.
Vdovykin, G. (1970) Ureilites. Space Science Reviews, 10, 483–510.

Manuscript received October 15, 2020
Manuscript accepted March 3, 2021
Manuscript handled by Simon A.T. Redfern